Noncovalently Assembled Electroconductive Hydrogel

Xu, Y.; Yang, X.; Thomas, A. K.; Patsis, P. A.; Kurth, T.; Kräter, M.; Eckert, K.; Bornhäuser, M.; Zhang, Y.;

Originally published:

April 2018

ACS Applied Materials and Interfaces 10(2018)17, 14418-14425

DOI: https://doi.org/10.1021/acsami.8b01029

Perma-Link to Publication Repository of HZDR:

https://www.hzdr.de/publications/Publ-27229

Non-covalently Assembled Electroconductive Hydrogel

Journal:	*ACS Applied Materials & Interfaces*
Manuscript ID	am-2018-01029c.R1
Manuscript Type:	Article
Date Submitted by the Author:	16-Mar-2018
Complete List of Authors:	Xu, Yong; B CUBE Center for Molecular Bioengineering, Technische Universität Dresden Yang, Xuegeng; Helmholtz-Zentrum Dresden-Rossendorf, Institute of Fluid Dynamics Thomas, Alvin; B CUBE Center for Molecular Bioengineering, Technische Universität Dresden Patsis, Panagiotis A; B CUBE Center for Molecular Bioengineering, Technische Universität Dresden Kurth, Thomas; Technische Universität Dresden ,DFG-Center for Regenerative Therapies Dresden Kräter, Martin; University Hospital Carl Gustav Carus der Technischen Universität Dresden, Medizinische Klinik und Poliklinik I Eckert, Kerstin; Helmholtz-Zentrum Dresden-Rossendorf (HZDR), Institute of Fluid Dynamics Bornhauser, Martin; Universitätsklinikum Carl Gustav Carus, Medizinische Klinik und Poliklinik 1 Zhang, Yixin; B CUBE - Center for Molecular Bioengineering, Technische Universität Dresden,

Non-covalently Assembled Electroconductive Hydrogel

Yong Xu,[†] Xuegeng Yang,[‡] Alvin Kuriakose Thomas,[†] Panagiotis A. Patsis, [†] Thomas Kurth,[§]

Martin Kräter, [‖] Kerstin Eckert,[‡] Martin Bornhäuser, [‖] Yixin Zhang*,[†]

[†]B CUBE Center for Molecular Bioengineering, Technische Universität Dresden, 01307 Dresden, Germany
[‡]Helmholtz-Zentrum Dresden-Rossendorf (HZDR), Institute of Fluid Dynamics, Dresden, Germany
[§] Technische Universität Dresden, DFG-Center for Regenerative Therapies Dresden.
[‖]University Hospital Carl Gustav Carus der Technischen Universität Dresden, Medizinische Klinik und Poliklinik I, Fetscherstraße 74, 01307 Dresden, Germany

ABSTRACT Crosslinking biomolecules with electroconductive nanostructures through non-covalent interaction can result in modular networks with defined biological functions and physical properties such as electric conductivity and viscoelasticity. Moreover, the resulting matrices can exhibit interesting features caused by the dynamic assembly process, such as self-healing and molecular ordering. In this paper, we present a physical hydrogel system formed by mixing peptide-polyethylene glycol and poly(3,4-ethylenedioxythiophene) polystyrene sulfonate (PEDOT:PSS). This combinatorial approach, which uses different modular building blocks, could lead to high tunability on aspects of rheology and electrical impedance. The proposed physical hydrogel system is characterized by both a self-healing ability and injectability. Interestingly, the formation of hydrogels at relatively low concentrations led to a network of closer molecular packing of PEDOT nanoparticles, reflected by the enhanced conductivity. The biopolymer system can be used to develop 3D cell cultures with incorporated electric stimuli, as evidenced by its contribution to the survival and proliferation of encapsulated mesenchymal stromal cells and their differentiation upon electrical stimulation.

KEYWORDS: *self-assembling, PEDOT:PSS, peptide, electroconductive hydrogel, 3D cell culture, electrical stimulation*

INTRODUCTION

Electroconductive biopolymers have shown great potential across a wide range of biomedical applications, including neuroprostheses, biosensors, nerve grafts and drug delivery.[1–5] Developments in polymerization methods and post-polymerization modification/grafting techniques have enabled the development of soft functional matters, which can be engineered to fulfill desired mechanical, electrical, and biochemical demands.[6–10] By developing electroconductive polymers that mimic the extracellular matrix (ECM) structures researchers aim to combine the biochemical and dynamic features of native tissue with electronic properties, resulting in the seamless electronic-biological interface. The attributes of the network that arise from reversible non-covalent interactions are important for many biomedical applications, such as the generation of shear-thinning and self-healing.[11–13] Moreover, a non-covalently assembled network using modular building blocks can enable the production of generalizable platforms with tunable mechanophysical, electrochemical and biochemical properties.[10,14] To reduce the complexity of the ECM to a non-covalently assembled synthetic matrix with modular and chemically defined components, we have previously developed a physical hydrogel system based on the interaction between a minimal peptide motif ((KA)n or (RA)n) and negatively charged oligosaccharides.[15–18] By varying the peptide and sulfated oligosaccharide (*e.g.*, dextran sulfate (DS), heparin) components, the non-covalent networks can be tailored for applications such as 3D cell culture and drug release. Importantly, the dynamic network showed shear-thinning and self-healing abilities, properties that are essential for injectability. In mice, injected hydrogels have shown high compatibility and did not cause adverse inflammatory responses.[18] As poly(3,4-ethylenedioxythiophene) polystyrene sulfonate (PEDOT:PSS), a widely used conductive polymer, is also highly negatively charged due to the excess PSS,[19] it could be incorporated into non-

covalently assembled matrices, for generating conductive biomaterials (Figure 1A and B). Moreover, we hypothesized that its use could lead to a tunable modular system possessing a structure-function relationship between peptide sequences, polymer linkage and the mechanical, electronic and cell adhesive properties.

To this end, we synthesized CWGG(BX)n peptides (KA7, KA5, KA3, KS7, KG7, RA7, RG7), where B is a basic residue (either arginine or lysine) and X is alanine, glycine or serine (Figure 1A). The thiol group of cysteine was used to link the peptides to maleimide-functionalized PEG by Michael-type addition reactions, while tryptophan was used to facilitate monitoring during HPLC purification and NMR quantification (Figure S1-S4). We first tested whether the sulfated oligosaccharide could be replaced by PEDOT:PSS to form a stable hydrogel. KA7-starPEG in PBS was mixed with PEDOT:PSS aqueous solution to final concentrations of 2.5 mM and 1 %, respectively. Different from the KA7-starPEG/heparin or KA7-starPEG/DS systems, which gelated slowly and formed homogeneous hydrogels, KA7-starPEG/PEDOT:PSS gelated instantly. Consequently, gel formation was too fast for efficient mixing, resulting in an inhomogeneous hydrogel. The same was observed for KA5-starPEG/PEDOT:PSS and RA7-starPEG/PEDOT:PSS. While KG7-starPEG/heparin did not form a hydrogel,[15] KG7-starPEG/PEDOT:PSS also gelated instantly, forming an inhomogeneous hydrogel. These results indicate that PEDOT:PSS provides stronger interactions than heparin and DS for the assembly of peptide-polymer into a non-covalent network. As KA7 connected to linear PEG-10k formed a very weak hydrogel (storage modulus < 10 Pa) with heparin, we tested hydrogel formation by mixing KA7-PEG-5k, KA7-PEG-10k, or KA7-PEG-20k with PEDOT:PSS. Interestingly, the gelation rates were slower than that of KA7-starPEG/PEDOT:PSS and efficient mixing led to the formation of homogeneous hydrogels.

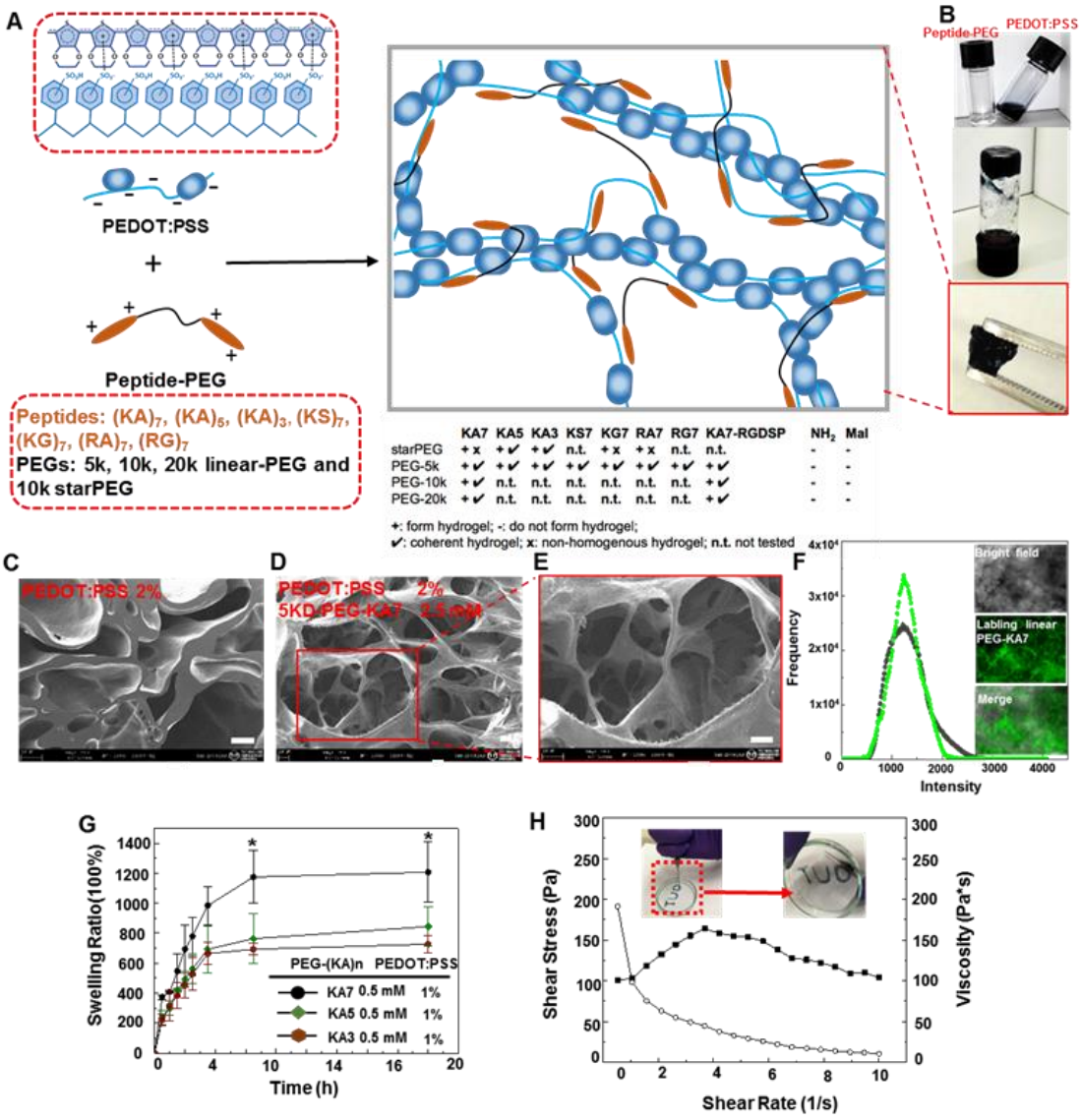

Figure 1. Characteristics of electroconductive PEDOT:PSS/peptide-PEG hydrogels. A) Assembly of peptide-PEG and negatively charged PEDOT:PSS nanostructures, resulting in a non-covalent network. In addition to the peptide:PSS interaction, the π–π stacking among PEDOT nanoparticles and the anion−π interaction between PEDOT and PSS are also involved in the non-covalent network. B) Representative hydrogel formation by mixing PEDOT:PSS and KA7-PEG-5k solutions. C) SEM image of lyophilized PEDOT:PSS. Scale bar: 100 μm. D and E) SEM images of conductive hydrogel (2.5 mM KA7-PEG-5k and 2% PEDOT:PSS). Scale bar: 100 μm. F) Hydrogel pixel density distribution of bright field images and fluorescein-labeled linear PEG KA7 (insets: upper, bright field image; middle: fluorescein image of 5KD linear-PEG KA7; bottom: merge image). G) Swelling of vacuum-dried conductive hydrogels in PBS buffer at 37 ℃. H) Continuous flow experiments showing the shear stress (closed symbols) and viscosity (open symbols) of hydrogel (0.5 mM KA7-PEG-5k and 1% PEDOT:PSS. Inset: The hydrogel is syringe-injectable and can adhere to glass when holding the dish vertically). n = 3; mean ± s.d.; * $p < 0.05$ for KA7 hydrogels compared to KA3 hydrogels.

While branched polymers can increase the crosslinking degree, linear PEGs possess narrower molecular weight distribution. Moreover, it is relatively easy to separate a linear PEG chain with two peptides from those with only one peptide, as evidenced by the purification of the star PEG with four peptides from a mixture with lower degree of modification. Therefore, in the present study, we investigated hydrogel formation using linear peptide-PEGs. As shown in Figure 1A, when coupled to PEG-5k, KA7, KA5, KA3, KS7, KG7, RA7 and RG7, PEDOT:PSS formed homogeneous hydrogels. In addition to the peptide:PSS interaction, the π–π stacking among PEDOT nanoparticles [19] and the anion−π interaction (Figure S18) between PEDOT and PSS are also involved in the non-covalent network. To incorporate a cell adhesive ligand into the network, we added the RGDSP sequence to the KA7 peptide. The resulting KA7-RGDSP-PEG-5k, KA7-RGDSP-PEG-10k, and KA7-RGDSP-PEG-20k formed homogeneous hydrogels with PEDOT:PSS.

Like the hydrogels obtained using sulfated oligosaccharides, the PEDOT:PSS containing hydrogels are very stable. No degradation was observed after incubating the biomaterials in PBS buffer or cell culture medium over a period of up to six months. The hydrogels were also resistant to harsh conditions such as deionized water, Dimethylformamide (DMF), Dimethyl sulfoxide (DMSO), ethanol, 1 M HCl, and 1 M NaOH (Figure S5). While the addition of TFE (trifluoroethanol) to KA7-starPEG/heparin hydrogel dissolved the matrix immediately by destroying the α-helical structure of KA7, treating KA7-PEG-5k/PEDOS:PSS hydrogel with TFE caused the hydrogel to break into fragile pieces. Together with the rheological studies discussed later, these results indicate that the secondary structure of KA7 is beneficial but not essential for forming a stable hydrogel with PEDOT:PSS. When KA7-PEG-5k is less than 2.5 mM in the presence of 1 % PEDOT:PSS, the resulting hydrogel is smaller than the combined volume after

mixing the two components, forming a layer of supernatant above the hydrogel. The syneresis effect reflects the minimum cross-linking density required for the non-covalent network. Freeze-drying is a pore-protecting drying method, which is widely used to process hydrogels for SEM imaging.[20] The PEDOT hydrogel displayed a typical 3D interconnected porous structure, compared to the freeze-dried PEDOT:PSS which had a smoother surface (Figure 1C-E). The non-covalent hydrogels remained intact after vacuum drying while increasing the number of KA repeats led to high cationic charge densities, promoting the use of large needles (Figure 1G).

To demonstrate that the injectable material possesses shear-thinning and self-healing properties, we performed continuous flow experiments and step-strain rheological studies using the KA7-PEG-5k/PEDOT:PSS hydrogel. The shear rate was linearly ramped from 0 to 10 s^{-1} to investigate the effect of shear rate on viscosity and shear stress. The hydrogel formed by mixing 0.5 mM KA7-PEG-5k and 1 % PEDOT:PSS (Figure 1 H) showed the desired shear thinning behavior, whereas the viscosity decreased with the shear rate. Consequently, shear stress increased to a maximum and then decreased slowly, which has been previously examined in various supramolecular networks and determined to be a consequence of network rearrangement and non-covalent interaction during the high shear rate induced flow.[21,22] In developing injectable hydrogels for biomedical applications, such drastic shear thinning behavior is advantageous as it increases the materials' ability to flow through narrow gauge needles.[23,24] After forming a hydrogel by mixing 2.5 mM KA7-PEG-5k and 1 % PEDOT:PSS, strong strain was applied to break the hydrogel, and the recovery of storage modulus was followed under 25 ℃ and 37 ℃. As shown in figure 2C, instant recovery of hydrogel characteristic (G' >> G'') was observed once the applied strain was removed. Full recovery of stiffness occurred after approximately 20 min. The self-healing capacity of hydrogel was also tested macroscopically. The hydrogel formed by mixing 2.5 mM KA7-PEG-

5k and 1 % PEDOT:PSS was cut into four pieces in an aqueous solution, which were then placed together (Figure 2C). After 10 min, the sample self-healed and could be lifted by tweezers. A possible self-healing mechanism is shown in figure 2D. The non-covalent interaction between the peptide and PSS allows the reversible breaking and recovery of the hydrogel network. The fast self-healing may also benefit from the hydrophobic interaction among PEDOT nanoparticles and the anion−π interaction between PSS and PEDOT.[19]

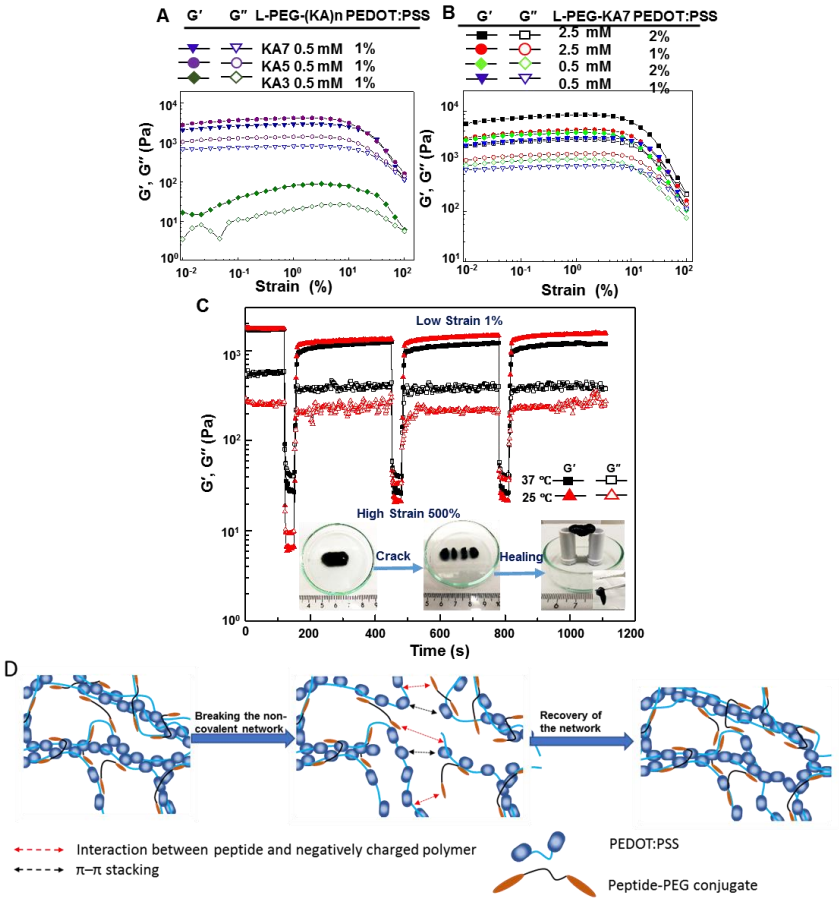

Figure 2. Rheological properties of the electroconductive hydrogel. A-B) Amplitude sweep performed after the hydrogel gelated for 1 h, with a frequency of 1 Hz and shear strain increasing from 1% to 100%; each test was repeated three times. C) The self-healing property when the alternate step strain was switched from 1% to 500% under different temperatures (25 ℃ and 37 ℃). Insets are images showing the self-healing of the hydrogel. The hydrogel was cut into four pieces, put together and healed into one block. D) Scheme of the self-healing process of the conductive hydrogel.

By varying the peptide-PEG and the concentrations of individual components, the mechanic properties could be tuned. We performed rheological studies to investigate the structure-function relationship between the chemical composition of the modular system and its mechanical properties. By increasing the number of (BX)n repeats (Figure 2A and Figure S9), the storage modulus increased gradually. KA7-PEG-5k/PEDOT:PSS and KA5-PEG-5k/PEDOT:PSS hydrogels exhibited storage moduli of 5,000 Pa and 3,000 Pa, respectively, while the KA3-PEG-5k/PEDOT:PSS hydrogel was remarkably softer (20 Pa). Subsequently, we tested the influence of different polymer chains on the hydrogel mechanic properties. Reducing the length of the PEG chain caused an increase in the storage modulus. The KA7-PEG-5k/PEDOT:PSS hydrogel is remarkably stiffer than the KA7-PEG-10k/PEDOT:PSS and KA7-PEG-20k/PEDOT:PSS hydrogels (Figure S9 C-D). Shortening the polymer chain caused a more densely crosslinked network. As expected, increasing the concentrations of KA7-PEG-5k and PEDOT:PSS enhanced the storage modulus. The hydrogel formed by mixing 2.5 mM and 2 % PEDOT:PSS had a storage modulus of 10,000 Pa while lowering the concentrations of KA7-PEG-5k and PEDOT:PSS to 0.5 mM and 0.5 %, respectively, remarkably reduced the storage modulus (Figure 2B and Figure S9A). While the $(BA)_n$ motif is essential for the gelation of the peptide-starPEG/heparin system, KG7-PEG-5k can also be used to form hydrogels with PEDOT:PSS. Nevertheless, the use of the KG7 peptide remarkably reduced the storage modulus (Figure S10 B and D). The hydrogel can also be compressed by the tweezers and instantly recovered its original geometry again with water, showing a shape memory behavior (Movie S1). With the same concentrations of peptide-PEG and PEDOT:PSS, KA7-PEG/PEDOT:PSS hydrogel has shown the highest stiffness, as compared with KG7, RA7 and RG7. Given that the stiffness of hydrogels can be tuned by varying the

concentrations, we can cover the largest range of stiffness by using KA7-PEG. Therefore, we focused on KA7 peptide in the following study.

While the modularity of the peptide-polymer system can be used to tune its mechanical properties, we also investigated whether it could allow us to incorporate additional biochemical cues. The integrin binding peptide RGDSP has been widely used as a biopolymer modification to enhance cell adhesion.[25] KA7-RGDSP-PEG-5k was synthesized and was able to form a hydrogel with PEDOT:PSS. However, the resulting hydrogel had a reduced storage modulus of 200 Pa (Figure S10 A and C), as compared to the KA7-PEG-5k/PEDOT:PSS hydrogel. To investigate the hydrogels at elevated temperatures, for applications including mammalian cell culture and implantation, we performed storage modulus *versus* temperature scans (Figure S11). The stiffness of the KA7-PEG-5k/PEDOT:PSS hydrogel decreased when the temperature was increased to 50 ℃, whereas the hydrogel characteristic (G' >> G'') were preserved through the temperature scan.

We then investigated the effect of various building blocks on the electrochemical properties of the hydrogel. Cyclic voltammetry (CV) curves of the hydrogels were typical of PEDOT:PSS-based materials when scanned over the range of -0.4 to 0.8 V, at a scan rate of 10 mV s^{-1} (Figure 3A), showing the oxidation peak between 0.5 V and 0.7 V, with reduction occurring between -0.1 V and -0.02 V (Figure 3A). Interestingly, when decreasing the concentration of PEDOT: PSS, both the anodic and cathodic currents increased significantly. Cyclic voltammograms obtained from the electrode with 1 % PEDOT:PSS had higher current densities for both oxidation and reduction compared with those of the 2 % PEDOT:PSS. Moreover, the oxidation and reduction peaks varied directly and inversely, respectively, with the scan rate (Figure 3B), which is attributed to the decreased electrode resistance with the increase in scan rate. By increasing the number of (KA)n repeats (Figure S13B and S14B), the impedance decreased gradually. KA7-PEG-5k/PEDOT:PSS

hydrogel exhibited an impedance of 35 Ω, while KA3-PEG-5k/PEDOT:PSS and KA5-PEG-5k/PEDOT:PSS hydrogels had an even higher resistance. Subsequently, we tested the influence of different polymer chains on the electrochemical properties of the hydrogel. Changing the PEG chain length had little influence on conductivity. KA7-PEG-5k/PEDOT:PSS, KA7-PEG-10k/PEDOT:PSS and KA7-PEG-20k/PEDOT:PSS hydrogels (Figure S13A and S14A) showed impedance in a similar range.

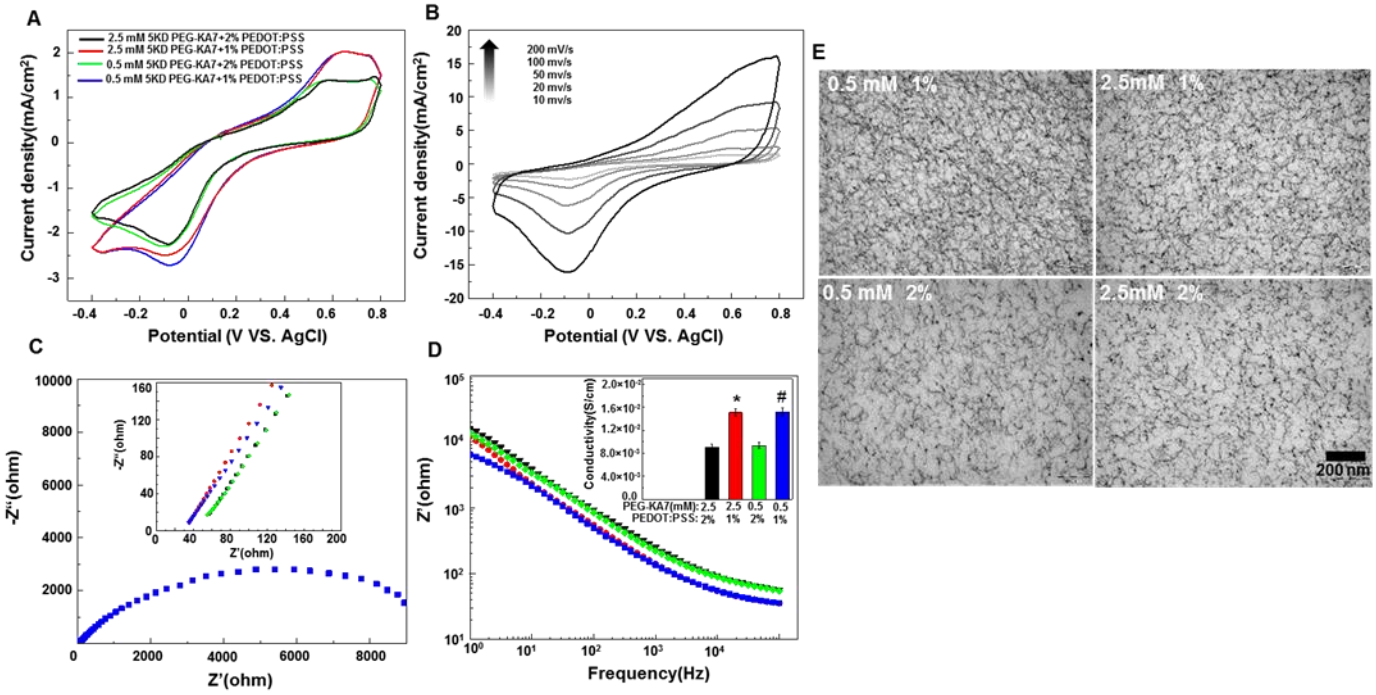

Figure 3. A) Cyclic voltammograms of hydrogels containing different concentrations of KA7-PEG-5k and PEDOT:PSS in 0.1 M PBS at a scan rate of 10 $mV.s^{-1}$. B) Cyclic voltammograms of hydrogel (0.5 mM KA7-PEG-5k and 1 % PEDOT: PSS) in PBS, at different scan rates. C) Nyquist plot of hydrogel (0.5 mM KA7-PEG-5k and 1 % PEDOT: PSS) (inset: the spectra of Nyquist plots of hydrogels with different concentrations of KA7-PEG-5k and PEDOT:PSS). D) Electrochemical impedance spectroscopy (Z *vs*. frequency) of conductive hydrogels with different concentrations of KA7-PEG-5k and PEDOT:PSS (inset: the conductivity of hydrogels with different concentrations). E) TEM images of conductive hydrogels with different concentrations of KA7-PEG-5k and PEDOT:PSS. The colors of plots in A, C and D are the same. n = 3; mean ± s.d.; * $p < 0.05$ for 2.5 mM KA7-PEG-5k and 1 % PEDOT:PSS hydrogels compared to 2.5 mM KA7-PEG-5k and 2 % PEDOT:PSS hydrogels; # $p < 0.05$ for 0.5 mM KA7-PEG-5k and 1 % PEDOT:PSS hydrogels compared to 0.5 mM KA7-PEG-5k and 2 % PEDOT:PSS hydrogels.

The non-covalently cross-linked network is important for the electroconductive behavior.[10] As compared with solutions of either KA7-PEG or PEDOT:PSS, the impedance is remarkably lower for the KA7-PEG-5k/PEDOT:PSS hydrogel (Figure S19). Interestingly, lowering the concentration of PEDOT:PSS decreased the impedance of the non-covalently assembled matrix (Figure 3C and 3D). The result was also confirmed by the CV measurements (Figure 3A). In the network, electron mobility is governed not only by the number of the conductive nanoparticles but also by the arrangement of the conjugated system and dopant. Although containing fewer conductive nanoparticles, the matrix with 1 % PEDOT:PSS and 0.5 mM KA7-PEG-5k showed a significant decrease in impedance compared to the hydrogel formed by mixing 2 % PEDOT:PSS and 2.5 mM KA7-PEG-5k. Transmission electron microscopy (TEM) revealed heterogeneous and porous nanostructures (Figure 3E). While the micrometer-sized structures are denser, the hydrogels formed at high concentrations (*e.g.*, 2.5 mM KA7-PEG-5k and 2 % PEDOT:PSS) exhibit thicker peripheral shells compared to the hydrogels formed at low concentrations (Figure S20;*e.g.*, 0.5 mM KA7-PEG-5k and 1 % PEDOT:PSS). However, the network connectivity of hydrogel formed at high concentrations is remarkably inferior to the well-connected dense matrix formed at low concentrations. The difference in conductivity is associated with the difference in connectivity of the assembled nanostructures.

Subsequently, we tested the utility of the conductive hydrogel system in developing 3D cell cultures. PEGylated PEDOT:PSS nanoparticles have been previously shown to exert diminished cytotoxicity, enabling the development of a novel drug delivery platform.[26] Moreover, because the gelation process does not involve any organic or electrochemical reactions, cells can be easily encapsulated into the matrix through a simple mixing procedure. Mesenchymal stromal cells (MSCs) were cultured on KA7-PEG-5k/PEDOT:PSS and RGDSP-KA7-PEG-5k/PEDOT:PSS

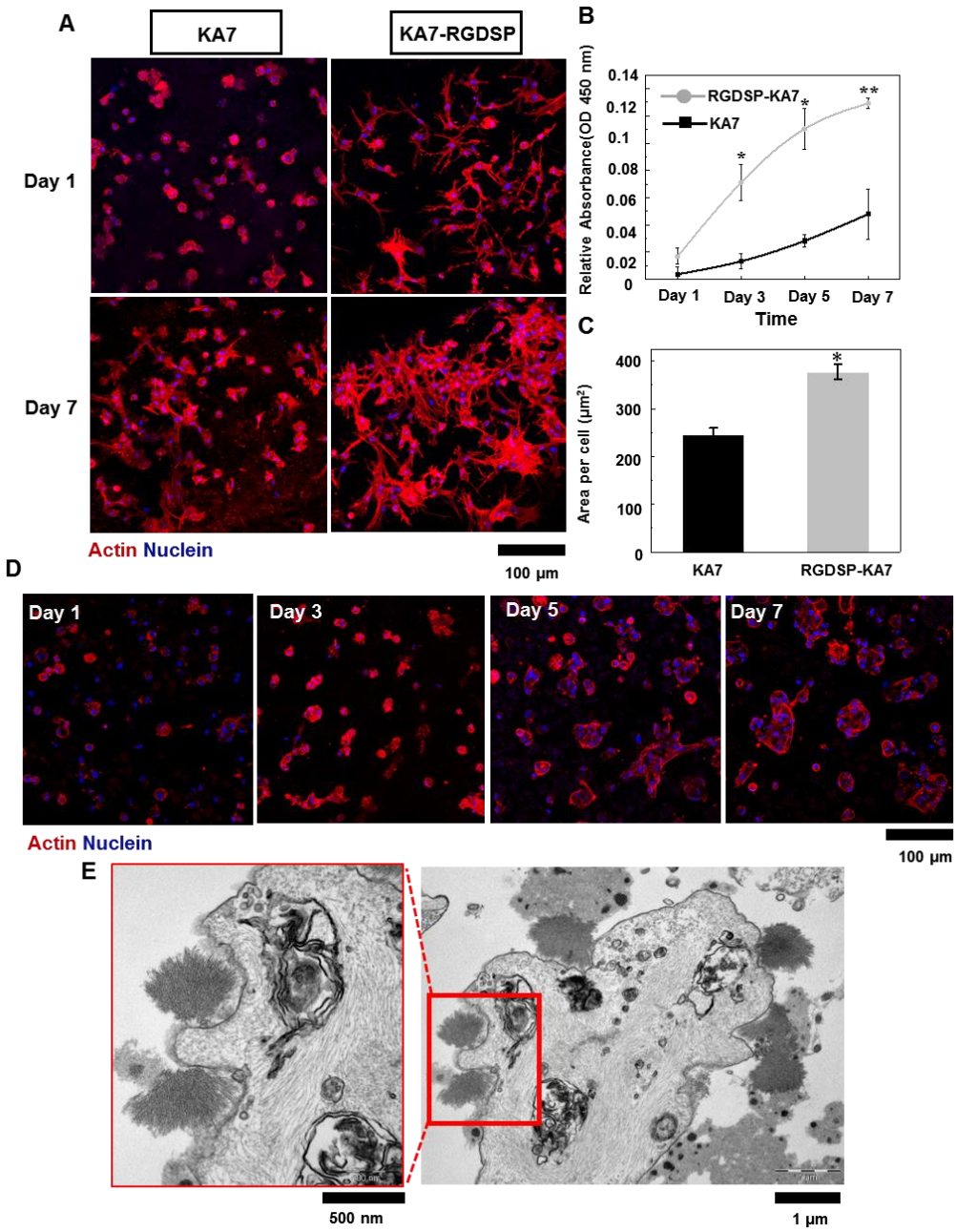

Figure 4. A) Confocal microscope images of MSCs on hydrogels with 0.5 mM KA7-PEG-5k or KA7-RGDSP-PEG-5k and 1% PEDOT:PSS, at day 1 and day 7. B) Proliferation of MSCs cultured on hydrogels at day 1, 3, 5 and 7. C) The area of MSCs on hydrogels at day 1. D) Confocal microscope images of MSCs in hydrogels at day 1, 3, 5 and 7. E) TEM images of MSCs encapsulated in the 0.5 mM KA7-PEG-5k and 1% PEDOT:PSS hydrogels at day 5. n = 3; mean ± s.d.; * $p < 0.05$,** $p < 0.01$ for RGDSPKA7-PEG-5k hydrogels compared to KA7-PEG-5k hydrogels.

hydrogels, and the presence of the RGDSP peptide remarkably improved cell adhesion (Figure 4A-C). The conductive hydrogel also supported the survival and growth of cells when these were

encapsulated in the non-covalent matrix (Figure 4D and Figure S15, S16). One day after embedding MSCs in the KA7-PEG-5k/PEDOT:PSS hydrogel, cells dispersed evenly in the 3D matrix. After 5 and 7 days of culture, an increasing number of spheric colonies became detectable.

Electrical stimulation (ES) can affect the development and regeneration of many tissues.[27–29] Therefore, we investigated MSC differentiation under ES. MSCs premixed with PEDOT:PSS in culture medium were added to KA7-PEG-5k on indium tin oxide (ITO)-coated glass slides (Figure 5A). The cell-laden hydrogels were then subjected to ES over a period of 10 days by applying short pulses (2 ms of 500 mV at 4 ms intervals, for 8 hours daily). From day 5 onwards, some cells began exhibiting changes in morphology when ES was applied. Interestingly, there was little change in conductivity during the first 4 days (Figure 5B), while the measured current increased gradually after day 5, which coincided with the gradual changes in cell morphology. This indicates that the non-covalently assembled conductive matrix can not only provide a seamless cell-material interface for applying ES to cells in 3D but may also be responsive to changes in the biological environment around the cells. TEM showed a marked change in matrix network upon MSC embedding (Figure 4E). The formation of nanofiber bundles could be observed around the cells. This indicates that the increase in conductivity is associated with the rearrangement of nanostructures caused by the presence and growth of the cells, while the underlying biological and chemical mechanisms remain to be determined.

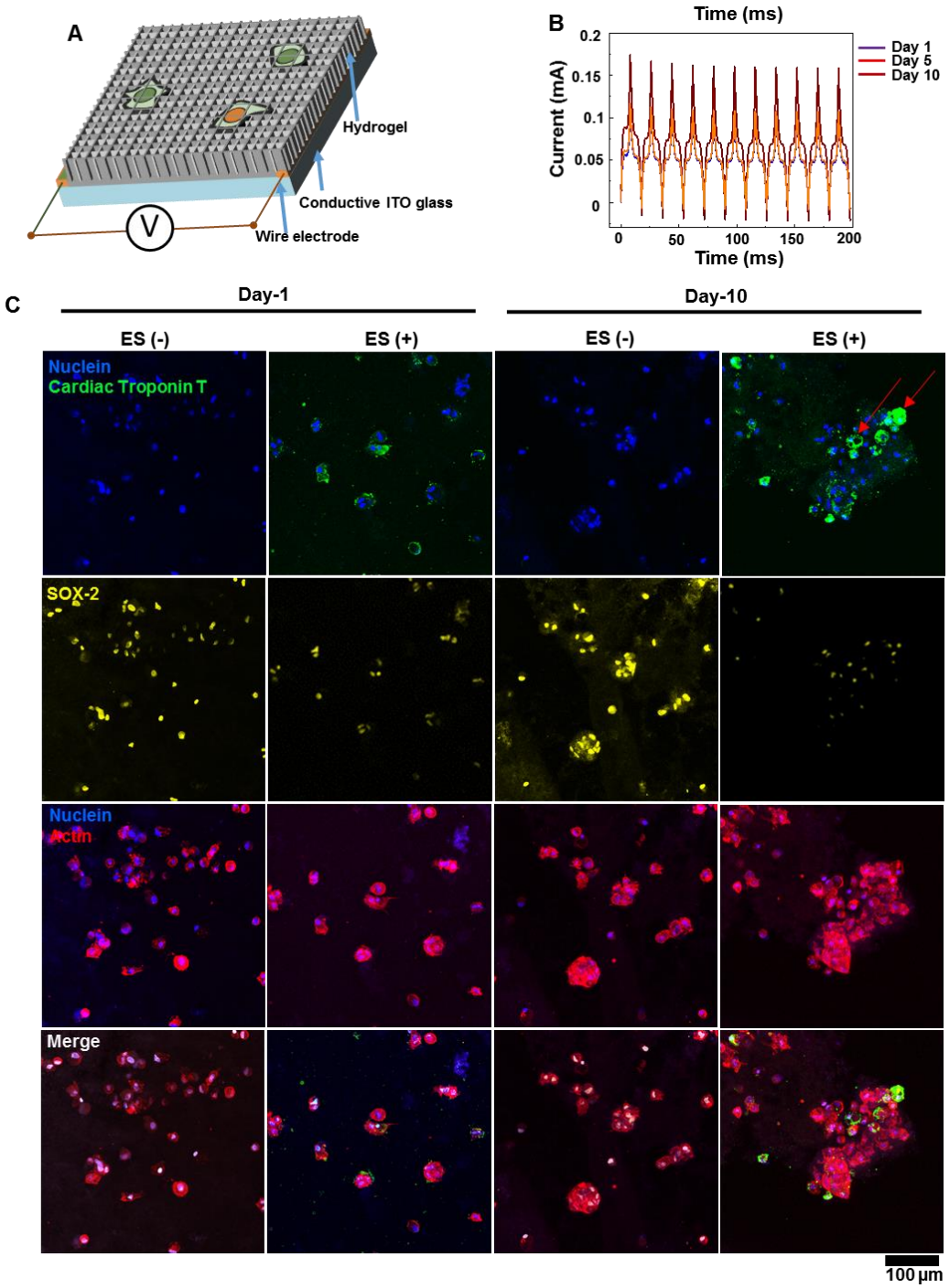

Figure 5. A) Schematic representation of the electrical stimulation of encapsulated MSCs in the 0.5 mM KA7-PEG-5k and 1% PEDOT:PSS hydrogels. B) The pulse current of continuous electrical stimulation at days 1, 5 and 7. C) cTnT and SOX-2 immunofluorescence staining of MSCs cultured on 0.5 mM KA7-PEG-5k and 1% PEDOT:PSS hydrogels at days 1 and 10. ES (−): without electrical stimulation; ES (+): with electrical stimulation.

In addition to the gradual change in morphology, ES-treated MSCs also exhibited remarkable up-regulation of the myocardiocyte marker cardiac troponin T (cTnT) (Figure 5C). MSCs in hydrogels were fixed 1 and 10 days after encapsulation and probed by the anti-cTnT antibody. Interestingly, one day after encapsulation, although the morphology of ES-treated cells was undistinguishable from that of control cells (without ES treatment), cTnT expression was only observed in ES-treated cells. After 10 days of culture under ES treatment, MSCs exhibited high expression of cTnT, while the untreated cells remained cTnT-negative. In contrast, the expression of the pluripotency marker SOX-2 was diminished upon ES. While the nature of the encapsulated cells remains to be further characterized, untreated MSCs developed into mesensphere-like structures, whereas ES caused cells to differentiate into myocardiocyte-like cells.

The underlying mechanism regarding how cells sense the conductive materials and respond to ES remains to be investigated in the future. A major drawback of the peptide-PEG/PEDOT:PSS system is that it cannot be easily degraded, preventing us from characterizing the cells with some methods commonly used in cell biology (e.g., cytometry). The dark materials are also not ideal for microscope imaging. A major challenge is to develop degradable conductive hydrogels, which would allow us to release the cells from the conductive 3D matrices (with or without ES), and investigate the impacts on signal transduction.

CONCLUSIONS

In summary, we developed a modular system to generate an electroconductive hydrogel through a non-covalent assembling approach, aiming to combine the ECM-mimicking matrix with organic electronics. Different from most conductive polymers, gelation through non-covalent interaction does not involve any organic or electrochemical reactions. While both the mechanical and electronic properties can be tuned by altering the modular structures, the dynamic network

also presents self-healing properties. Electron mobility in the 3D network is governed not only by the concentration of conductive polymer but also by the arrangement of the nanostructures, which can be affected by the assembling conditions, as well as by the growth of encapsulated cells. The system can be used to develop 3D cell cultures with incorporated ES function, as shown by its support of the survival and proliferation of encapsulated MSCs and their differentiation under ES.

ASSOCIATED CONTENT

Supporting Information

Experimental procedures, chemical syntheses, mechanical analysis, stability, electrochemical testing, cell culture. This material is available free of charge *via* the Internet at http://pubs.acs.org.

AUTHOR INFORMATION

Corresponding Author

yixin.zhang1@tu-dresden.de

Notes

The authors declare no competing financial interests.

ACKNOWLEDGMENTS

The authors thank Ulrike Hofmann for technical support on peptide synthesis and Markus Günther for SEM imaging. The authors thank Dr. Hella Hartmann and Silke White for LSM imaging. Meiying Cui and Kejun Liu provided help with image collection and FTIR measurements. We thank N. Kröger and A. Kotzsch for helps in DLS measurements .This work was supported by the China Scholarship Council and the German Federal Ministry of Research and Education (BMBF grants 03Z2EN12 and 03Z2E511).

REFERENCES

(1) Wang, Q.; Cheng, H.; Peng, H.; Zhou, H.; Li, P. Y.; Langer, R. Non-Genetic Engineering of Cells for Drug Delivery and Cell-Based Therapy. *Adv. Drug Deliv. Rev.* **2015**, *91*, 125–140.

(2) Feiner, R.; Dvir, T. Tissue–electronics Interfaces: From Implantable Devices to Engineered Tissues. *Nat. Rev. Mater.* **2017**, *3*, 17076.

(3) Harris, A. R.; Wallace, G. G. Organic Electrodes and Communications with Excitable Cells. *Adv. Funct. Mater.* **2017**, *1700587*, 1–23.

(4) Shi, Z.; Gao, X.; Wajid, M.; Li, S.; Wang, Q. Biomaterials Electroconductive Natural Polymer-Based Hydrogels. *Biomaterials* **2016**, *111*, 40–54.

(5) Balint, R.; Cassidy, N. J.; Cartmell, S. H. Conductive Polymers: Towards a Smart Biomaterial for Tissue Engineering. *Acta Biomater.* **2014**, *10*, 2341–2353.

(6) Dong, R.; Zhao, X.; Guo, B.; Ma, P. X. Self-Healing Conductive Injectable Hydrogels with Antibacterial Activity as Cell Delivery Carrier for Cardiac Cell Therapy. *ACS Appl. Mater. Interfaces* **2016**, *8*, 17138–17150.

(7) Zhao, X.; Wu, H.; Guo, B.; Dong, R.; Qiu, Y.; Ma, P. X. Antibacterial Anti-Oxidant Electroactive Injectable Hydrogel as Self-Healing Wound Dressing with Hemostasis and Adhesiveness for Cutaneous Wound Healing. *Biomaterials* **2017**, *122*, 34–47.

(8) Zhao, X.; Guo, B.; Ma, P. X. Single Component Thermo-Gelling Electroactive Hydrogels from Poly(caprolactone)–poly(ethylene Glycol)–poly(caprolactone)-Graft-Aniline Tetramer Amphiphilic Copolymers. *J. Mater. Chem. B* **2015**, *3*, 8459–8468.

(9) Zhao, X.; Li, P.; Guo, B.; Ma, P. X. Antibacterial and Conductive Injectable Hydrogels Based on Quaternized Chitosan-Graft-Polyaniline/oxidized Dextran for Tissue Engineering. *Acta Biomater.* **2015**, *26*, 236–248.

(10) Wu, Y.; Guo, B.; Ma, P. X. Injectable Electroactive Hydrogels Formed via Host-Guest Interactions. *ACS Macro Lett.* **2014**, *3*, 1145–1150.

(11) Raeburn, J.; Zamith Cardoso, A.; Adams, D. J. The Importance of the Self-Assembly Process to Control Mechanical Properties of Low Molecular Weight Hydrogels. *Chem. Soc. Rev.* **2013**, *42*, 5143–5156.

(12) Goktas, M.; Cinar, G.; Orujalipoor, I.; Ide, S.; Tekinay, A. B.; Guler, M. O. Self-Assembled Peptide Amphiphile Nanofibers and PEG Composite Hydrogels as Tunable ECM Mimetic Microenvironment. *Biomacromolecules* **2015**, *16*, 1247–1258.

(13) Fichman, G.; Gazit, E. Self-Assembly of Short Peptides to Form Hydrogels: Design of Building Blocks, Physical Properties and Technological Applications. *Acta Biomaterialia*, 2014, *10*, 1671–1682.

(14) Deng, Z.; Guo, Y.; Zhao, X.; Ma, P. X.; Guo, B. Multifunctional Stimuli-Responsive Hydrogels with Self-Healing, High Conductivity, and Rapid Recovery through Host–Guest Interactions. *Chem. Mater.* **2018**, acs.chemmater. 30, 1729−1742.

(15) Wieduwild, R.; Tsurkan, M.; Chwalek, K.; Murawala, P.; Nowak, M.; Freudenberg, U.; Neinhuis, C.; Werner, C.; Zhang, Y. Minimal Peptide Motif for Non-Covalent Peptide-Heparin Hydrogels. *J. Am. Chem. Soc.* **2013**, *135*, 2919–2922.

(16) Wieduwild, R.; Lin, W.; Boden, A.; Kretschmer, K.; Zhang, Y. A Repertoire of Peptide Tags for Controlled Drug Release from Injectable Noncovalent Hydrogel. *Biomacromolecules* **2014**, *15*, 2058–2066.

(17) Wieduwild, R.; Krishnan, S.; Chwalek, K.; Boden, A.; Nowak, M.; Drechsel, D.; Werner, C.; Zhang, Y. Noncovalent Hydrogel Beads as Microcarriers for Cell Culture. *Angew. Chemie - Int. Ed.* **2015**, *54*, 3962–3966.

(18) Tondera, C.; Wieduwild, R.; Röder, E.; Werner, C.; Zhang, Y.; Pietzsch, J. In Vivo Examination of an Injectable Hydrogel System Crosslinked by Peptide–Oligosaccharide Interaction in Immunocompetent Nude Mice. *Adv. Funct. Mater.* **2017**, *27*. 1605189

(19) Zhang, S.; Cicoira, F. Water-Enabled Healing of Conducting Polymer Films. *Adv. Mater.* **2017**, *29*, 1–6.

(20) Mukai, S. R.; Nishihara, H.; Tamon, H. Formation of Monolithic Silica Gel

Microhoneycombs (SMHs) Using Pseudosteady State Growth of Microstructural Ice Crystals. *Chem. Commun.* **2004**, 874-875.

(21) Appel, E. A.; Biedermann, F.; Rauwald, U.; Jones, S. T.; Zayed, J. M.; Scherman, O. A. Supramolecular Cross-Linked Networks via Host-Guest Complexation with cucurbit[8]uril. *J. Am. Chem. Soc.* **2010**, *132*, 14251–14260.

(22) Xu, D.; Hawk, J. L.; Loveless, D. M.; Jeon, S. L.; Craig, S. L. Mechanism of Shear Thickening in Reversibly Cross-Linked Supramolecular Polymer Networks. *Macromolecules* **2010**, *43*, 3556–3565.

(23) Rodell, C. B.; Kaminski, A.; Burdick, J. A. Rational Design of Network Properties in Guest-Host Assembled and Shear-Thinning Hyaluronic Acid Hydrogels. *Biomacromolecules* **2013**, *14*, 1–20.

(24) Rodell, C. B.; Dusaj, N. N.; Highley, C. B.; Burdick, J. A. Injectable and Cytocompatible Tough Double-Network Hydrogels through Tandem Supramolecular and Covalent Crosslinking. *Adv. Mater.* **2016**, 8419–8424.

(25) Hart, S. L.; Knight, A. M.; Harbottle, R. P.; Mistry, A.; Hunger, H. D.; Cutler, D. F.; Williamson, R.; Coutelle, C. Cell Binding and Internalization by Filamentous Phage Displaying a Cyclic Arg-Gly-Asp-Containing Peptide. *J. Biol. Chem.* **1994**, *269*, 12468–12474.

(26) Gong, H.; Cheng, L.; Xiang, J.; Xu, H.; Feng, L.; Shi, X.; Liu, Z. Near-Infrared Absorbing Polymeric Nanoparticles as a Versatile Drug Carrier for Cancer Combination Therapy. *Adv. Funct. Mater.* **2013**, *23*, 6059–6067.

(27) Yang, B.; Yao, F.; Hao, T.; Fang, W.; Ye, L.; Zhang, Y.; Wang, Y.; Li, J.; Wang, C. Development of Electrically Conductive Double-Network Hydrogels via One-Step Facile Strategy for Cardiac Tissue Engineering. *Adv. Healthc. Mater.* **2016**, *5*, 474–488.

(28) Mawad, D.; Mansfield, C.; Lauto, A.; Perbellini, F.; Nelson, G. W.; Tonkin, J.; Bello, S. O.; Carrad, D. J.; Micolich, A. P.; Mahat, M. M.; *et al.* A Conducting Polymer with Enhanced Electronic Stability Applied in Cardiac Models. *Sci. Adv.* **2016**, *2*, 1–13.

(29) Mooney, E.; Mackle, J. N.; Blond, D. J. P.; O'Cearbhaill, E.; Shaw, G.; Blau, W. J.; Barry, F. P.; Barron, V.; Murphy, J. M. The Electrical Stimulation of Carbon Nanotubes to Provide a Cardiomimetic Cue to MSCs. *Biomaterials* **2012**, *33*, 6132–6139.

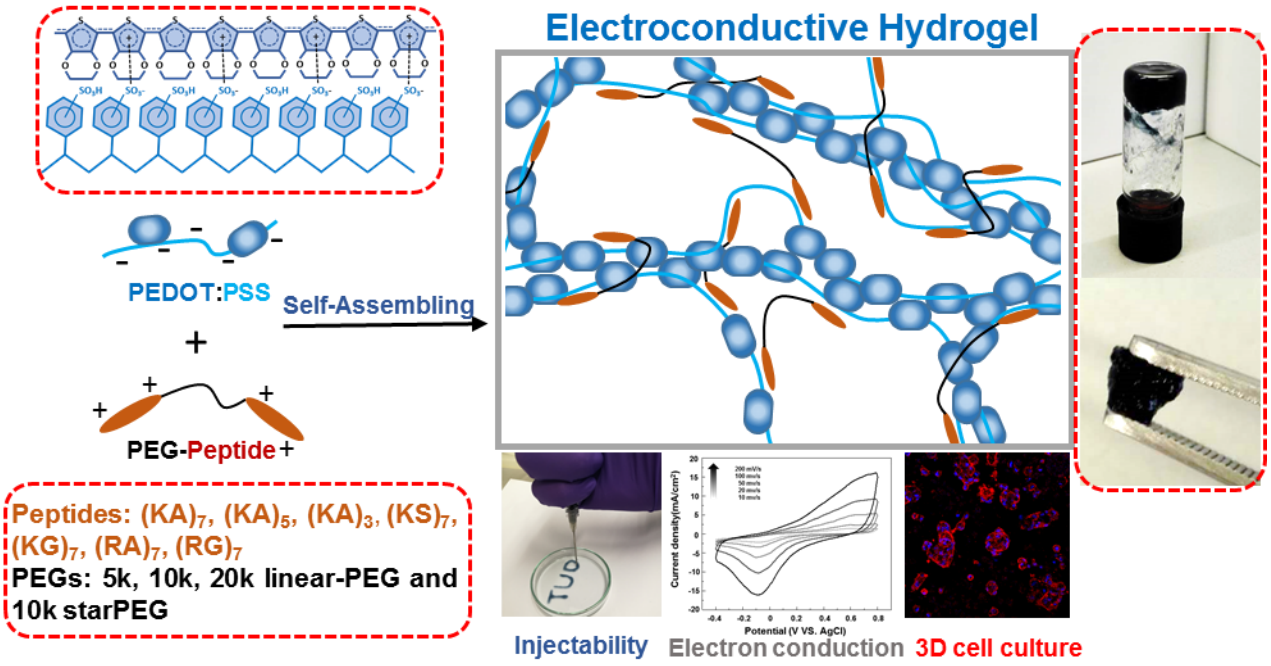
Electroconductive Hydrogel
PEDOT:PSS
Self-Assembling
PEG-Peptide
Peptides: $(KA)_7$, $(KA)_5$, $(KA)_3$, $(KS)_7$, $(KG)_7$, $(RA)_7$, $(RG)_7$
PEGs: 5k, 10k, 20k linear-PEG and 10k starPEG
Injectability
Electron conduction
3D cell culture